Free surface effects on thermodynamics and glass formation in simple monatomic supercooled liquids

V. V. Hoang[1,2,*] and T. Q. Dong[2]

[1]*Department of Physics, Institute of Technology, National University of Ho Chi Minh City, 268 Ly Thuong Kiet Street, District 10, Ho Chi Minh City, Vietnam*

[2]*Université de Marne-la-Vallée, Cité Descartes, Bât. Lavoisier, Champs-sur-Marne, 77454 Marne-la-Vallée, Cedex 2, France*

(Received 5 August 2011; published 9 November 2011)

Free surface effects on the thermodynamics and glass formation in simple monatomic supercooled liquids with the Lennard-Jones–Gauss interaction potential were studied by the molecular dynamics simulations. Glass with two free surfaces was obtained by cooling from the melt. We found the following important new results: Free surfaces significantly enhance atomic mobility in the system compared to that of the bulk and induce the formation of so-called layer structure of the interior of both liquid and glassy states. A mobile surface layer in the system exists for a wide temperature range; i.e., the thickness of the mobile surface layer and the discrepancy between atomic mobility in the surface and that in the interior have a tendency to increase with temperature. The atomic mechanism of glass formation in supercooled liquids with free surfaces exhibits "heterogeneouslike" behavior, unlike the "homogeneous" behavior observed in the bulk; i.e., the solidlike "domain" initiates/enhances in the interior and simultaneously grows outward to the surface to form a glassy solid phase. The interior of glass with free surfaces exhibits a stronger local icosahedral order compared to that of the bulk, and it may lead to higher stability of the glassy state compared to that of the latter. In contrast, the surface shell has a more porous structure and contains a large number of undercoordinated sites.

DOI: 10.1103/PhysRevB.84.174204 PACS number(s): 64.70.Q−, 61.43.Fs, 64.70.P−

I. INTRODUCTION

Glass with free surfaces (with or without interface with the substrate, i.e., thin film–like glass) has been under intensive investigation by both experiments[1–45] and computer simulations or theoretical models[46–64] for decades due to its scientific and technological importance. While experiments have focused on the fabrication and the interfacial and confinement-induced properties of glassy thin films, theoretical models or computer simulations have tried to get more detailed information at the atomistic level of the surface structure, mechanism of glass formation, and dynamics or thermodynamics of the systems. Study of glassy thin films, including the effects of free surfaces or interfaces on their structure and properties, remains an active research area. Recently, it was found that glassy thin films obtained by vapor deposition can be highly stable (henceforth referred to as "stable glass") compared to ordinary glass obtained by quenching from the melt.[18] This discovery provided the impetus for further research in this direction.[21–23,29,30,33,36,39,40,42–45] Stable glass exhibits lower enthalpy and higher density compared to ordinary glass. It was suggested that high-mobility molecules within a few nanometers of the surface have time to find low-energy packing configurations before they are buried by further deposition and that this leads to the formation of an ultrastable glassy state.[18,22] Optical photobleaching experiments revealed the existence of two subsets of probe molecules with different dynamics in stable glass, which can be explained by the existence of a high-mobility layer at the surface of glassy films.[43] Similarly, the existence of glass with a liquidlike layer was previously suggested, although it has been under debate.[6] An enhanced mobility surface is an important problem, relevant for adhesion, friction, coatings, and nanoscaled fabrication such as etching and lithography.[56] Stable glassy thin film of toluene and ethylbenzene were also obtained by vapor deposition.[65–67]

Although some theoretical models or simulations were done to clarify various aspects of thin glassy films in the past, they mainly focused on confined polymeric thin film models.[46–64] Recently, a schematic-facilitated kinetic Ising model was proposed that is capable of reproducing the key experimentally observed characteristics of vapor-deposited stable glass.[61] Furthermore, an atomistic molecular model of trehalose was used for examination of properties of vapor-deposited stable glass.[62] These simulations supported the Ediger group's argument that surface-induced high mobility during the deposition process is the mechanism of formation of stable glass.[18] Properties of the atomic freestanding thin films of a binary Lennard-Jones (LJ) mixture have been studied by molecular dynamics (MD) simulations, and it was suggested that surface atoms are able to sample the underlying energy landscape more effectively than those in the interior, which may be related to the mechanism of formation of stable glass.[63] We are carrying out a research project of various substances in models with free surfaces via MD simulations to highlight the situation. In the present work, we show the results for Lennard-Jones–Gauss (LJG) glass with free surfaces. Details about the calculations can be seen in Sec. II. Results and discussions about the thermodynamics, evolution of the structure, and atomic mechanism of glass formation in a system with free surfaces can be found in Sec. III. Conclusions are given in the last section of the paper. Using simple monatomic models, we can easily monitor the atomic mechanism of phase transitions or related phenomena, since we can focus on the topological order of the atomic arrangements only, rather than on both topological and chemical orders, as is necessary if we use binary systems.

II. CALCULATIONS

Glass formation and related thermodynamics have been studied in models containing 5832 identical atoms interacting via the LJG potential:[68–72]

$$V(r)=\varepsilon\left[\left(\frac{\sigma}{r}\right)^{12}-2\left(\frac{\sigma}{r}\right)^{6}\right]-1.5\varepsilon\exp\left[-\frac{(r-1.47\sigma)^2}{0.04\sigma^2}\right]. \quad (1)$$

The LJG potential is a sum of the Lennard-Jones potential and a Gaussian contribution. The three-dimensional (3D) glassy state with an LJG potential remains unchanged after long annealing for 1093 ns (see Ref. 73), making it a very long-lived simple monatomic glassy model compared to those with LJ or Dzugutov potentials.[74,75] The following LJ-reduced units were used in the present work: length in units of σ, temperature T in units of ε/k_B, and time in units of $\tau_0=\sigma\sqrt{m/\varepsilon}$. Here, k_B is the Boltzmann constant, σ is an atomic diameter, and m is an atomic mass (for Ar, we have $m=0.66\times10^{-25}$ kg, $\varepsilon/k_B=118$ K, $\sigma=3.84$ Å; therefore, $\tau_0=\sigma\sqrt{m/\varepsilon}=2.44$ ps). The Verlet algorithm is employed, and the MD time step is $dt=0.001\tau_0$, or 2.44 fs if we are taking Ar for testing. A cutoff is applied to the LJG potential at $r=2.5\sigma$ like that used in Refs. 69–73. The initial configuration of a simple cubic structure at the density $\rho_0=0.8$ is melted in a cube of the length $L=19.39\sigma$ under periodic boundary conditions (PBCs) at a temperature as high as $T_0=2.0$ via MD relaxation for 2×10^5 MD steps. After that, PBCs are applied only in the x and y Cartesian directions, while in the z Cartesian direction, nonperiodic boundaries with an elastic reflection behavior are employed after adding the empty space of a length of $\Delta z=3\sigma$ at $z=L=19.39\sigma$. Due to using the elastic reflection boundaries, an additional free surface first occurs at $z=0.0$ during further MD simulation. The system is left to equilibrate further for 5×10^4 MD steps at $T_0=2.0$ at a constant volume corresponding to the new boundaries (i.e., NVT ensemble simulation). Then the system is cooled at the constant volume and temperature is decreased linearly with time as $T=T_0-\gamma\times n$ by simple atomic velocity rescaling. The cooling rate $\gamma=10^{-6}$ per 1 MD step (or 4.836×10^{10} K/s if we are taking Ar for testing) is used; n is the number of MD steps. To calculate the coordination number, Honeycutt-Andersen bond pair analysis, or clustering of atoms, we assume that two atoms located within the cutoff radius $R_o=1.25$ are neighbors. Here, the cutoff distance is the position of the minimum after the first peak in radial distribution function (RDF) for the glassy state obtained at $T=0.1$. To improve the statistics, we average the results over two independent runs.

III. RESULTS AND DISCUSSIONS

A. Thermodynamics

Temperature dependence of the inherent intermediate scattering function $F_S(Q,t)$, mean-squared displacement (MSD) of atoms, potential energy per atom, and diffusion constant are presented in Fig. 1. In the present work, $F_S(Q,t)$ is calculated for $Q=8.665\sigma^{-1}$, which is the location of the first peak in the structure factor $S(Q)$ of the bulk.[73] The function form is

$$F_S(Q,t)=\frac{1}{N}\sum_{j=1}^{N}\langle\exp(i\,Q.[r_j(t)-r_j(0)]\rangle, \quad (2)$$

where $r_j(t)$ is the location of the jth atom at time t and Q is a wave vector. We can see in Fig. 1(a) that $F_S(Q,t)$ is typical for supercooled glass-forming systems.[76,77] At high temperature, $F_S(Q,t)$ has the ballistic regime of motion of atoms at the short beginning time, followed by a relaxation behavior regime that is basically exponential and function decays to 0 within 1 τ_0. However, with further decreasing temperature, it has a tendency to form a plateau regime after the ballistic one and longer time portion of the curves exhibits nonexponential behavior like that found for various glass-forming supercooled liquids.[73,76,77] The plateau regime is related to the caging effects, i.e., the temporary trapping of atoms by their neighbors. We also found that details of slowing, as well as the shape of $F_S(Q,t)$, in the system with free surfaces are very different from the behavior of the bulk [see the curves for $T=1.5$ in Fig. 1(a)] yet like those found for thin polymer film.[50] Furthermore, we can see in Fig. 1(b) that the MSD has three regimes: the ballistic regime at the beginning of motion; followed by the plateau regime, which is related to the caging effects; and finally the diffusive regime over a longer time. These three regimes are seen clearly at low temperatures. It seems that the MSD of atoms in our system also has an additional regime: the saturation regime of a diffusion length of the calculation shell in the z direction. This fourth regime can be seen more clearly at high temperatures [Fig. 1(b)], like those found in nanoparticles.[72] The potential energy in the models with free surfaces is significantly higher than that of the bulk due to the surface contribution, and the starting point of deviation from the linearity of the low temperature region is a glass transition temperature [$T_g=0.61$, Fig. 1(c)]. Indeed, at $T\leqslant0.60$, atomic motion exhibits solidlike behavior; i.e., after the ballistic regime at the beginning, the motion of atoms enters the plateau regime for a long time, indicating a strong caging effect of a relatively rigid glassy state [Figs. 1(a) and 1(b)]. Due to the free surfaces, a significant number of atoms remain liquidlike in the glassy matrix, especially in the surface shell, leading to enhancement of MSD for a long time for a temperature just below $T_g=0.61$ [Fig. 1(b)].

A free surface or interface can greatly enhance the dynamics of atoms in the systems, according to evidence from experiments[4,6,7,17,19,26,30,33,35,38,41,43,45] or from computer simulations and theoretical models.[49,50,56,61–64] The diffusion constant (D) is found via the following Einstein relation:

$$\lim_{t\to\infty}\frac{\partial\langle\Delta r^2(t)\rangle}{6\partial t}=D. \quad (3)$$

Here, $\langle\Delta r^2(t)\rangle$ is the MSD of the atom. We show the inverse temperature dependence of the logarithm of the diffusion constant in Fig. 1(d). We can see that the diffusion constant in the system with free surfaces is always larger than that in the bulk for the whole temperature range studied. In particular, the discrepancy is of some orders of magnitude at the lowest temperature calculated [Fig. 1(d)]. At a high temperature, diffusion in both the bulk and the system with free surfaces follows an Arrhenius law, while at a low temperature, deviation

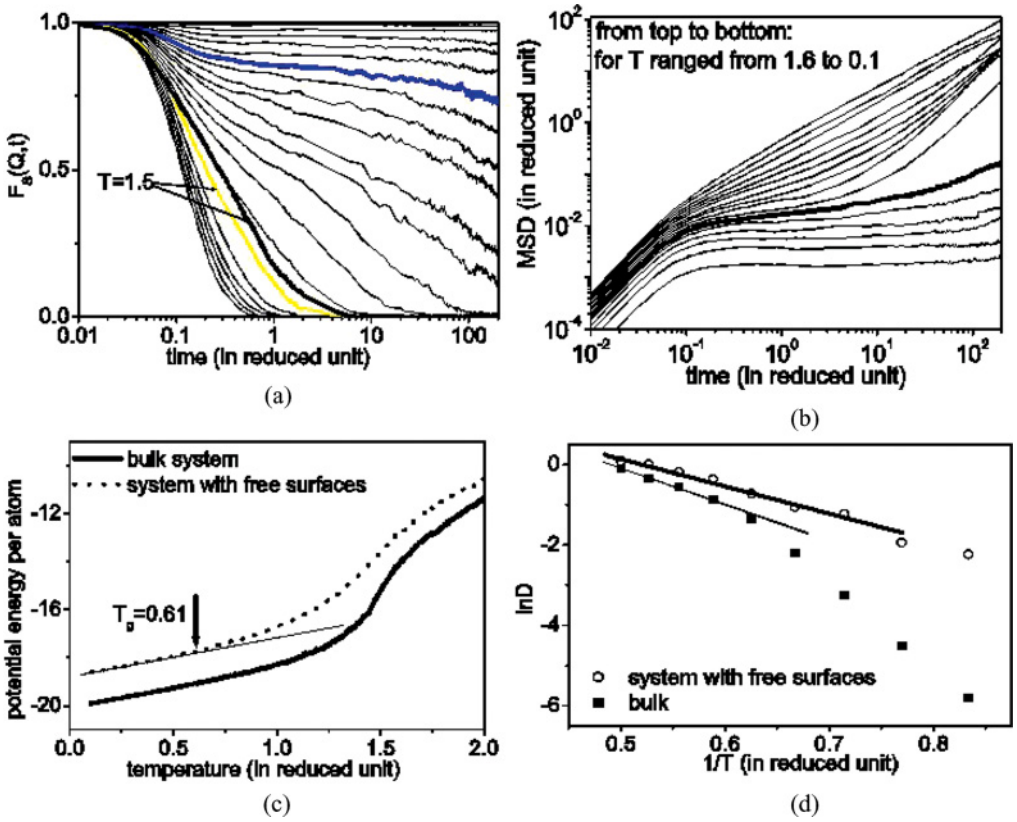

FIG. 1. (Color online) (a) Time–temperature dependence of the self-intermediate scattering function. From left to right, for temperatures ranging from $T = 2.0$ to $T = 0.1$, the yellow line is for the system with free surfaces at $T = 1.5$ compared to that of the bulk obtained at the same temperature (the bold line) (Ref. 73) and the thick blue line is for $T = 0.6$. (b) Time–temperature dependence of the MSD of atoms. The bold line is for $T = 0.6$. (c) Temperature dependence of the potential energy per atom in the system compared to that of the bulk (Ref. 71). The straight line is a visual guide. (d) Inverse temperature dependence of the logarithm of the diffusion constant in the system compared to that of the bulk (Ref. 71). The straight lines are visual guides.

from this law is found. However, deviation from an Arrhenius law is more pronounced for the bulk than for the system with free surfaces. This indicates free surface effects on the mechanism of diffusion in the system. It was found and discussed in Ref. 71 that the change in slope of the curve presented in Fig. 1(d) is related to the change in mechanism of diffusion from liquidlike to solidlike. Other researchers found that the lateral diffusion coefficient at the surface of the freestanding LJ thin film is roughly three times greater than at the center of the film.[63] In addition, they found that the diffusion constant and the velocity autocorrelation function in the center of the film match exactly the corresponding quantities of the bulk.

To get more detailed information about the local structure and dynamics in the system, we present the density profile and atomic displacement distribution (ADD) in the z direction in the models (Fig. 2). The density profile at a given temperature is calculated by partitioning the system in the z direction into slices of the thickness 0.2σ. Then we divide the number of atoms in each slice by the volume of a given slice. Similarly, ADD is found by dividing the total displacement of all atoms in the slice by the number of atoms in a given slice, and ADD corresponds to the displacement of atoms in the slice after a specific amount of time at a given temperature (τ_C), which was chosen appropriately. After intensive checking, we found that $\tau_C = 5\tau_0$ is a good choice (i.e., 12.2 ps or 5000 MD steps). We can see in Fig. 1(b) that this time is located at the end of a plateau regime for the MSD at T around a glass transition temperature (i.e., it is large enough for atoms to overcome a plateau regime to diffuse if it is a liquidlike one), and we use this time for calculating the Lindemann ratio (given later). To clarify the enhanced mobility of particles at the surface of the model of trehalose by measuring the Debye-Waller factor, it was argued that the characteristic time τ_C can be chosen appropriately depending on the physical phenomenon of interest.[62] Finally, a short period near the beginning of the caging regime equal to 10 ps was adopted since it provides a reasonable measure of the free volume in the system,[78,79] and is close to our $\tau_C = 12.2$ ps.

Some points can be drawn for the density profiles presented in Fig. 2. Density profile shows clearly that the system with free surfaces can be divided into two distinct parts: the surface shell and the interior. In the latter, the density profile shows a layer structure of orderly high and low values, and the layer structure is enhanced with decreasing temperature. However, density in the interior fluctuates around an average value for a given temperature, which increases with decreasing temperature, like that found for the binary LJ system.[63] In contrast, density in the surface shell decreases with distance from the interior, indicating a more porous structure in this part of the system

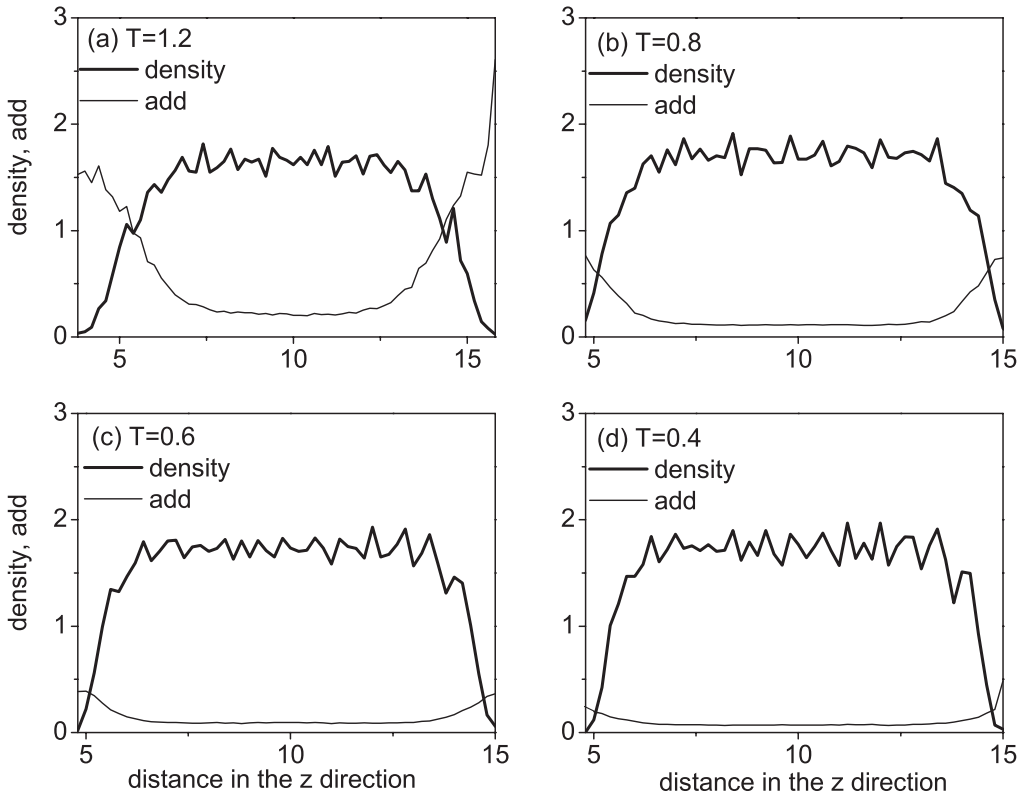

FIG. 2. Density profile and ADD the models obtained at different temperatures. For ADD, we employ the same scale as that for the density profile.

compared to that of the interior. We found a layer structure of the system for the whole temperature range studied (i.e., even at the highest temperature $T = 2.0$). Layering at the free liquid surfaces was also found for various systems.[80,81] It was argued that occurrence of the layer structure depends on the ratio T_m/T_C (T_C is a critical temperature for the system) and monatomic LJ liquid does not exhibit a layer structure.[80] A strong layer structure in the density profile was found for the molecular model of trehalose, and it was suggested to be the origin of the ultrahigh stability of vapor-deposited glass.[62]

In the z direction in the models, we can see that ADD also exhibits interior and surface behavior. In the interior ADD is rather constant at a low value, while in the surface shell it increases with distance from the interior (Fig. 2). Evidence of the existence of a high-mobility surface in glass with a free surface was found by both experiments and computer simulations. However, the phenomenon was only studied indirectly or partially, i.e., just via the Debye-Waller factor as a function of distance from the substrate layer[62] or via the lateral diffusion constant at two different temperatures.[63] There is a surface shell of enhanced mobility in our system (Fig. 2). The thickness of this layer d and the discrepancy between atomic mobility in the surface and that in the interior of the system h are determined as described in Fig. 3(a). The following important points can be listed: First, the thickness of the region of reduced density is almost the same as that for the region of enhanced mobility. However, it was suggested in the past that the latter should be an order of magnitude larger than the former.[6] Second, as shown in Fig. 3(b), the thickness of the mobile surface layer has a tendency to increase with temperature for the whole temperature range studied (i.e., from the glassy state to the normal liquid one) and shares some trends found for the liquid surface width of an isotropic dielectric liquid—i.e., tetrakis(2-ethoxyhexoxy)silane.[81] For the glassy region of polystyrene, d increases with temperature.[43] We found that a mobile surface layer exists for the whole temperature range studied and that it is new, since it was suggested that convergence of the surface and bulk dynamics should be complete at high temperatures (i.e., at $T > T_g + 5$ K for the freestanding polystyrene thin film[43]). Third, the discrepancy between atomic mobility in the interior and that in the surface shell also has a tendency to grow with temperature up to the normal liquid region [Fig. 3(c)]. Therefore, it does not support the suggestions that dynamics near surface has a weaker temperature dependence compared to dynamics in the interior and that the difference in the dynamics between the surface and the interior gets smaller as temperature approaches T_g from below.[43] Finally, the thickness of our models with free surfaces (in the z direction) decreases with decreasing temperature, leading to the formation of a glassy state with enhanced density in the interior (Fig. 2). This may lead to enhancement of stability of the obtained glassy state. It is also in accordance with stability observed for the freestanding thin film of the binary LJ mixture[63] or for the monatomic LJ system.[82] The quantity d is found by averaging of the results of two opposite sides. In addition, the mean density of the system increases with decreasing temperature, and the glass transition temperature (T_g) of the system can be found as the point of deviation from the linearity of the low temperature region [Fig. 3(d)]. A similar temperature dependence of density was

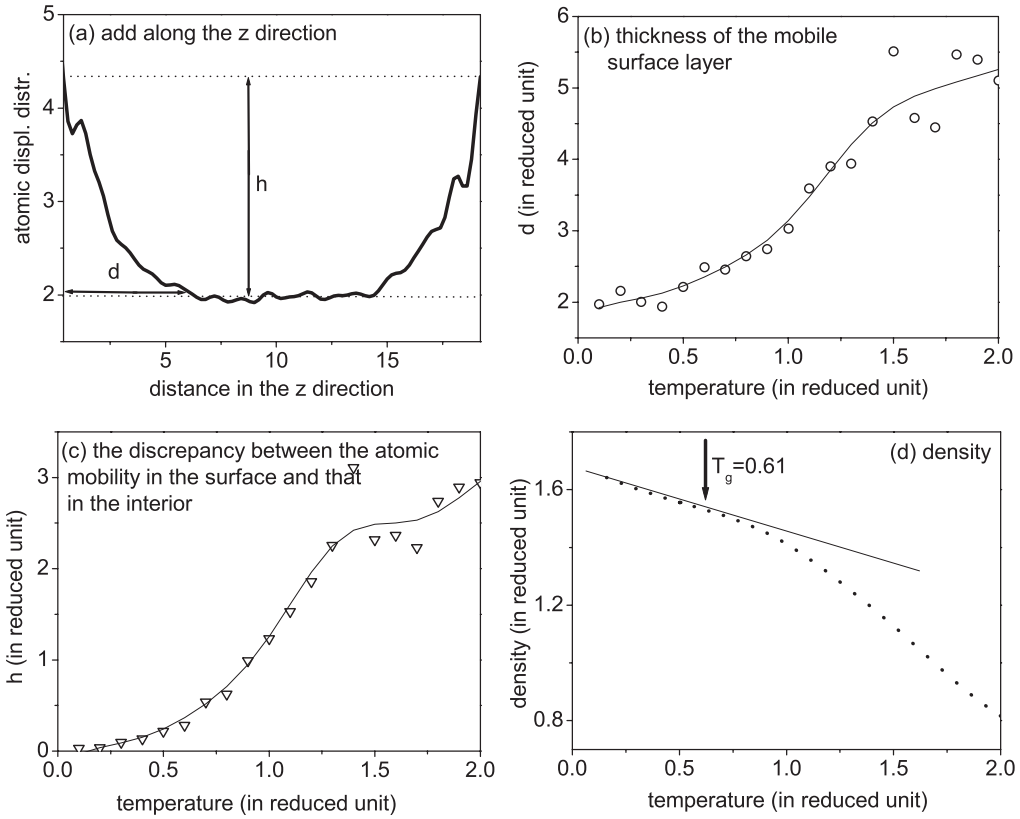

FIG. 3. (a) ADD in the model obtained at $T = 2.0$. The dotted lines and arrows are visual guides. We also show how to determine the discrepancy between atomic mobility in the surface and that in the interior of the system (denoted as h), as well as showing the thickness of the mobile surface layer (denoted as d). (b) Temperature dependence of the thickness of a mobile surface layer. The solid line is the averaged curve. (c) Temperature dependence of the discrepancy between mobility in the surface and that in the interior. Again, the solid line is the averaged curve. (d) Temperature dependence of the mean density of the system. The straight line is a visual guide.

found for the bulk, and the mean density of the system with free surfaces is slightly smaller than that of the bulk.[73]

B. Evolution of the structure upon cooling from the melt

It is of great interest to see the evolution of the structure of the system upon cooling from the melt. We can see in Fig. 4 that evolution of the RDF of the system is typical for glass-forming systems like those found and discussed.[69–75]

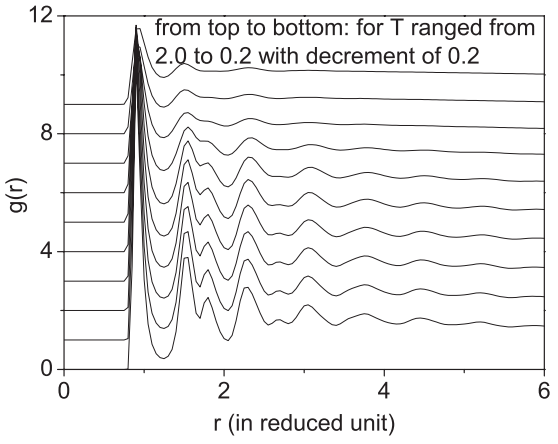

FIG. 4. RDF in the models obtained upon cooling from the melt.

We also show the coordination number distributions in the glassy model (at $T = 0.10$) compared to those of the bulk after the same relaxation for 2×10^5 MD steps (Fig. 5). The structure of interior of the system with free surfaces is close to that of the bulk, although the former has a more close-packed atomic arrangement compared to the latter (Fig. 5 and Table I). However, the surface shell of the models exhibits a

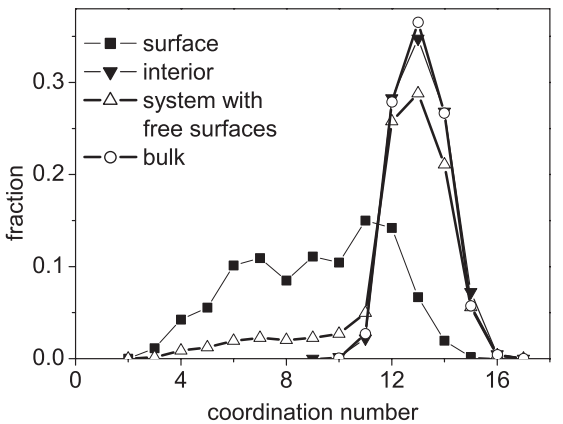

FIG. 5. Coordination number distributions in the well-relaxed model with free surfaces obtained at $T = 0.1$ compared to those of the bulk (Ref. 73).

TABLE I. Mean coordination number ($\overline{Z}$), mean interatomic distance ($\overline{R}$), glass transition temperature (T_g), and density (ρ) of the well-relaxed glassy system with free surfaces obtained at $T = 0.1$ compared to those of the bulk (Ref. 73). For glass with free surfaces, we show the averaged density.

Materials		$\overline{Z}$	$\overline{R}$	T_g	ρ
System with free surfaces	Surface	9.096			1.156
	Interior	13.096			1.765
	Whole	12.241	0.910	0.61	1.551
Bulk		13.030	0.900	1.00	1.759

non–close-packed atomic arrangement and contains a large number of undercoordinated sites (Table I). A high concentration of undercoordinated sites (or "structural defects" of glass) may be the origin of various surface phenomena of thin films.[13,83] For example, it was found that the well-relaxed silica surface contains a large number of structural defects, which can serve as reaction sites for the formation of silanols.[83] Still, Table I shows that the mean interatomic distance in LJG glass with free surfaces is somewhat larger than that of the bulk due to surface interatomic enhancement like that found for nanoparticles.[72] Free surfaces greatly reduce a glass transition temperature in the system from that of the bulk due to surface atomic–mobility enhancement (Table I). This tendency is consistent with that observed experimentally for thin films of various substances (e.g., Refs. 1 and 2). Glassy thin film models of trehalose obtained by "vapor deposition" also have a higher density, lower enthalpy, and higher onset temperature than corresponding "ordinary" glass formed by quenching the bulk liquid.[62] These glassy models of trehalose also contain a strong layer structure interior like that found in the present work. Moreover, it was found that the Fourier transformation of the local density profile of the trehalose models exhibits a pronounced peak.[62] This is reminiscent of the additional scattering peak reported by Dawson *et al*. for stable glass of indomethacin.[84] It was suggested that unusual properties of stable glass of indomethacin are the results of the layer structure interior of the samples induced by the formation process.[62]

The fraction of various bond pairs of the Honeycutt-Andersen analysis[70,73,85] in glass with free surfaces can be seen in Table II. According to the Honeycutt-Andersen analysis, structure is analyzed by the pairs of atoms on which four indices are assigned. The first index indicates whether or not they are near neighbors; thus, the first index is 1 if the pair is bonded and is 2 otherwise, where we used the fixed cutoff radius $R_o = 1.25$ for determining the nearest-neighbor pairs. The second index is equal to the number of near neighbors they have in common. The third index is equal to the number of bonds among common near neighbors. Finally, the fourth index denotes the existence of a structure with the same first three indices but with different arrangements.

Therefore, while the interior has a strong local icosahedral order and its relative fraction of bond pairs is close to that of the bulk, the surface shell contains a large number of bond pairs characteristic for non–close-packed atomic arrangements like those discussed previously by analyzing the coordination number distributions (Table II). We found that fraction of the 1551 bond pair in the interior is rather high like that found in metallic glass.[70,73,86,87] The 1551 pair is direct evidence of the existence of a local icosahedral order in the system.[85] This means that the energy-favored local structure of LJG glass is an icosahedral order, which is incompatible with global crystallographic symmetry. This is the origin of long-lived stability of LJG glass, since fivefold symmetry frustrates crystallization. However, the differences between bond-pair distributions in the interior and those in the bulk can be seen in Table II. That is, the fraction of the 1551 bond pair in the interior is higher than that in the bulk, and it may lead to higher stability against crystallization of glass with free surfaces. Experimental studies of stable glass have focused on macroscopic observables, and there is no detailed structural analysis in recent simulations of stable glassy models.[62,63] Therefore, it is difficult to determine the origin of their high stability.

The LJG interatomic potential used in the present simulations is a double well one.[68–70] For a two-dimensional system, it was found that the Gaussian part of the potential stabilizes the pentagonal configuration and packing of the pentagons produces frustration in crystallization of the obtained glass.[69] Moreover, competition of the two nearest-neighbor distances of a double-well interaction leads to the formation of 3D glass with a very high fraction of a local icosahedral order in the systems, in turn leading to high stability against crystallization.[70,73] The same situation is found in the present work for LJG glass with free surfaces.

C. Atomic mechanism of glass formation

To clarify the atomic mechanism of glass formation in supercooled liquids with free surfaces, the Lindemann-freezing–like criterion is used for detecting solidlike atoms occurring in the system upon cooling from the melt. Then we analyze their spatiotemporal arrangements. This procedure has been successfully used for determination of the atomic mechanism of glass formation in the bulk and nanoparticles.[71–73] The Lindemann ratio for the ith atom is[88]

$$\delta_i = \left\langle \Delta r_i^2 \right\rangle^{1/2} / \overline{R}. \quad (4)$$

TABLE II. Relative fraction of bond pairs in the well-relaxed glassy models with free surfaces compared to those of the bulk (Ref. 73) obtained at $T = 0.1$.

Models		1301	1311	1321	1421	1422	1441	1551	1541	1661
System with free surfaces	Surface	0.009	0.106	0.124	0.016	0.080	0.011	0.446	0.168	0.040
	Interior	0.002	0.013	0.022	0.017	0.030	0.030	0.598	0.198	0.089
Bulk		0.001	0.015	0.022	0.020	0.032	0.035	0.577	0.205	0.093

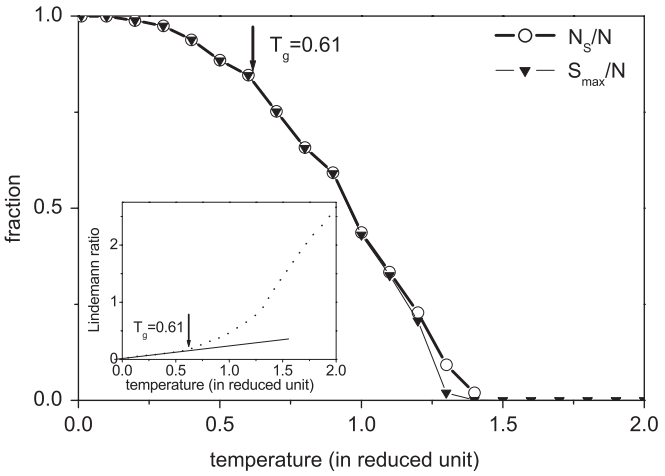

FIG. 6. Temperature dependence of the fraction of solidlike atoms (N_S/N) and size of the largest solidlike clusters ($S_{\max}/N$) to the total number of atoms in the system (N). The inset shows the temperature dependence of the Lindemann ratio.

Here, $\langle \Delta r_i^2 \rangle$ is the MSD of the ith atom and $\overline{R} = 0.91$ is an interatomic distance. For supercooled and glassy states, $\overline{R}$ does not change much with temperature, and we fix this value for the calculations. We define $\langle \Delta r_i^2 \rangle$ after a characteristic time τ_C as described previously, i.e., $\tau_C = 5\tau_0$ (5000 MD steps or 12.2 ps), and it is close to that found for the bulk and nanoparticles.[71–73] It was proposed that τ_C is not larger than some atomic vibrations in picoseconds.[89] We define the Lindemann ratio δ_L of the system by the average of δ_i over all atoms, $\delta_L = \sum_i \delta_i / N$. Temperature dependence of the Lindemann ratio can be seen in the inset of Fig. 6. We can see that the Lindemann ratio and potential energy show similar temperature dependence (Figs. 1 and 6), indicating a strong correlation between them in the vitrification process. That is, the starting point of deviation from the linearity of the low temperature region in Fig. 6 is a glass transition temperature. This means that $T_g = 0.61$ is determined exactly by the temperature dependence of three thermodynamic quantities: potential energy, density, and the Lindemann ratio. Moreover, $T_g = 0.61$ is a bound between liquidlike and solidlike dynamics in the system (see $F_S(Q,t)$ and the MSD in Fig. 1). We can see in Fig. 6 that at $T = T_g$, the Lindemann ratio has a critical value $\delta_C = 0.167$ and it is close to that found for the bulk and nanoparticles.[71–73] Therefore, atoms with $\delta_i \leqslant \delta_C$ are classified as solidlike, and atoms with $\delta_i > \delta_C$ are classified as liquidlike. A purely Lindemann criterion established that melting occurs when a root of MSD is at least 10% (usually ∼15%, which is close to our $\delta_C = 0.167$) of the atomic spacing.[88,90] Moreover, there is experimental evidence that this criterion is also applicable for glass.[91–93] The validity of the Lindemann criterion for melting and the glass transition was checked and confirmed recently.[90,94]

We found that the atomic mechanism of glass formation in the system with free surfaces shares some trends observed in the bulk.[71,73] That is, a significant number of solidlike atoms first occur around $T = 1.4$, at a point located somewhat lower than that of the bulk.[71,73] It may be due to free surfaces–induced mobility enhancement in the system. Furthermore, the number of solidlike atoms grows quickly with further cooling, and they have a tendency to form clusters [Fig. 6]. At the glass transition temperature ($T_g = 0.61$) ∼84% atoms in the system are solidlike to form a relatively rigid glassy phase. This fraction of solidlike atoms is close to that observed in the bulk and nanoparticles.[71–73] Further cooling leads to full solidification around $T_f = 0.10$, where the percentage of solidlike atoms is ∼100% (Fig. 6). We found that characteristic temperatures of glass formation in the system with free surfaces, i.e., T_g and T_f, are much smaller than those found in the bulk.[71,73] The tendency of solidlike atoms to form clusters can be seen via the curve of $S_{\max}/N$ in Fig. 6. That is, the size of the largest cluster $S_{\max}$ increases with decreasing temperature. Subsequently, around $T = 1.1$, the largest cluster contains almost 98% solidlike atoms in the system to form a thin film–like configuration (described later). Such a cluster can be considered percolated, like the one found in the bulk.[73] A single percolation cluster is formed by merging the small-size coarse clusters and single solidlike atoms when a fraction of solidlike atoms reaches a critical value p_C. We found here that $p_C = 0.33$ located within the range $0.15 \leqslant p_C \leqslant 0.45$, as suggested in Ref. 95. This means that glass formation in the system with free surfaces is also related to the percolation of solidlike clusters. However, percolation occurs at a temperature located well above the glass transition temperature, like the one found in the bulk and in nanoparticles.[71–73]

We also found some differences in glass formation in the system with free surfaces compared to that observed in the bulk. More details about the occurrence and clustering of solidlike atoms in supercooled liquids with free surfaces can be seen in the 3D visualization presented in Fig. 7. At the first stage of glass formation, solidlike atoms occur in the interior of the system, and their spatial distribution exhibits diversity behavior even though they have a tendency to form clusters [Fig. 7(a)]. The atomic configuration of solidlike clusters becomes more closely packed [Fig. 7(b)], and the configuration of a thin film shape is formed at a lower temperature [Fig. 7(c)]. This configuration of the thin film shape grows outward upon further cooling and forms a glassylike thin film at the temperature close to glass transition [Fig. 7(d)]. This means that glass formation in supercooled liquids with free surfaces exhibits "heterogeneouslike" behavior; i.e., the solidlike "domain" occurs/enhances in the interior and simultaneously grows outward to the surfaces. This is unlike the "homogeneous" glass formation observed in the bulk.[71,73] In addition, the lifetime of solidlike clusters in supercooled liquids with the LJG potential is rather long compared to the typical lifetime of ∼1 ps of the icosahedral cluster in the liquid Fe model obtained at 1900 K (see Ref. 96). It was found that the lower the temperature, the larger the solidlike clusters and the longer their lifetime.[71,73] A similar situation for the lifetime of solidlike clusters in models with free surfaces can be suggested.

The distributions of solidlike and liquidlike atoms in the z direction in the system during a vitrification process offer a more detailed picture of glass formation in the system (Fig. 8). Solidification of the system initiates/enhances in the interior and simultaneously grows outward [Figs. 8(a) and 8(b)]. Although liquidlike atoms distribute throughout the

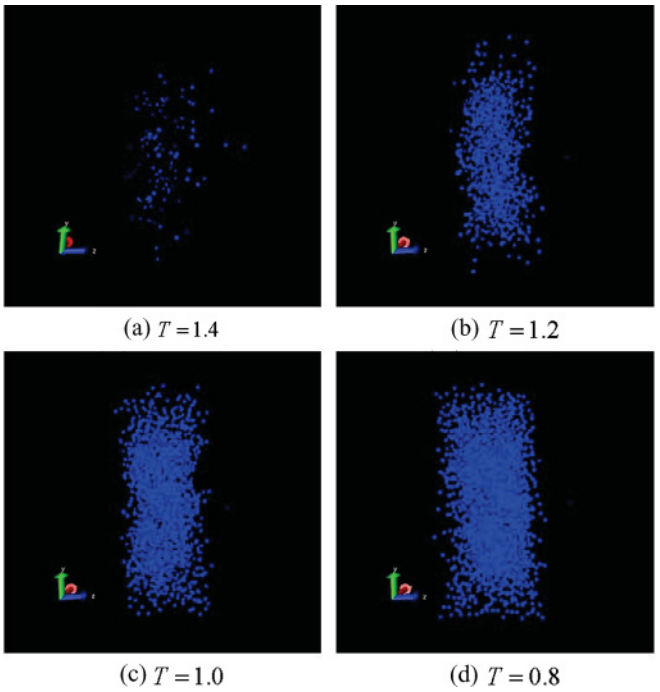

FIG. 7. (Color online) 3D visualization of the appearance of solidlike atoms in the system upon cooling from the melt.

system, they have a tendency to concentrate in the surface shell to form a liquidlike layer in the outermost part of the free surfaces [Figs. 8(b) and 8(c)]. However, at the glass transition temperature, the liquidlike surface layer disappears, and although liquidlike atoms still concentrate in the surface shell, their density is equal to that of solidlike atoms [Fig. 8(d)]. This means that we have a mixed phase of solidlike and liquidlike atoms with equal concentrations. The results of the present work highlight the debate about the existence of so-called glass with liquidlike surfaces[6] and give deeper understanding of glass formation in supercooled liquids with free surfaces. Moreover, this problem is reminiscent of the well-known phenomenon of surface premelting in solids,[6,97] and it is of great interest to check the nature of the so-called liquidlike surface layer of solids related to the premelting phenomenon.

Clarifying the nature of solidlike atoms occurring in the system upon cooling from the melt is helpful, since many things related to the nature of solidlike atoms (or solidlike domains) occurring in the supercooled region are still unclear.[98–101] To highlight the situation, we show in Fig. 9 the temperature dependence of the mean coordination number for solidlike and liquidlike atoms compared to that of the mean coordination number for all atoms in the system. We can see that the mean coordination number of solidlike atoms is always larger than that of all atoms; i.e., solidlike atoms often occur in the close-packed atomic arrangement regions. It is difficult for atoms located in the close-packed atomic arrangement regions to escape from their position; they are often trapped by their neighbors, and if the trapping time is long enough, they become solidlike. The number of solidlike atoms increases with decreasing temperature, and at a low temperature they dominate in the system. Therefore, the mean coordination number of solidlike atoms has a tendency to become closer to that of all atoms with decreasing temperature (Fig. 9). In

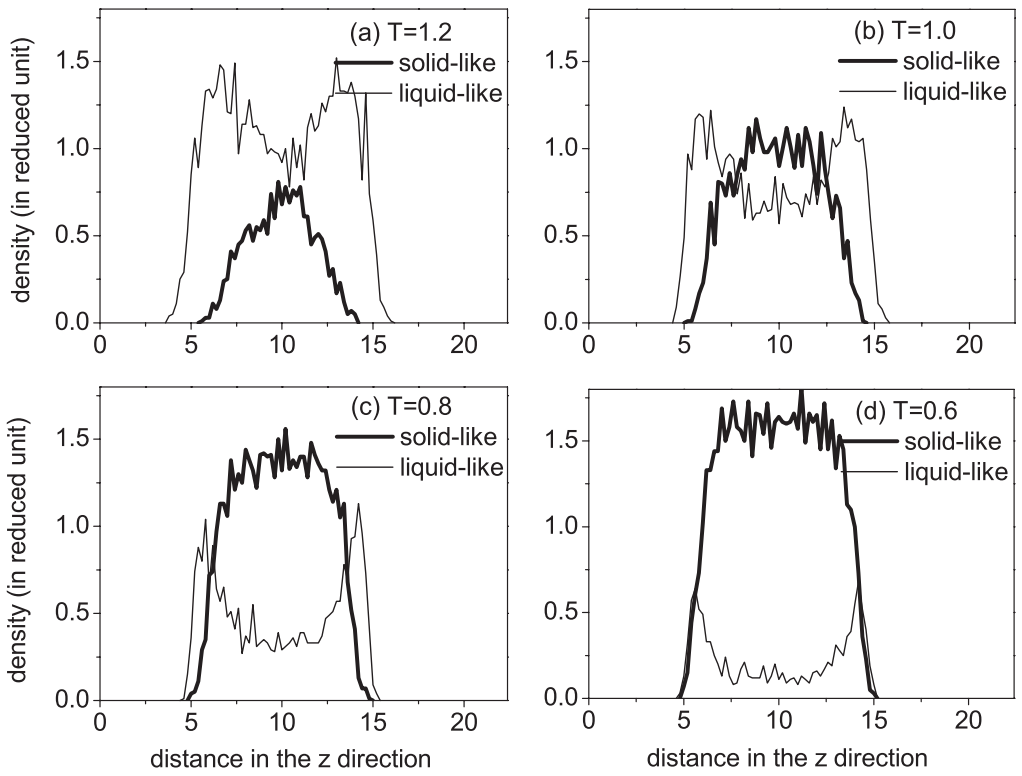

FIG. 8. Distributions of solidlike and liquidlike atoms in the z direction in models obtained at different temperatures.

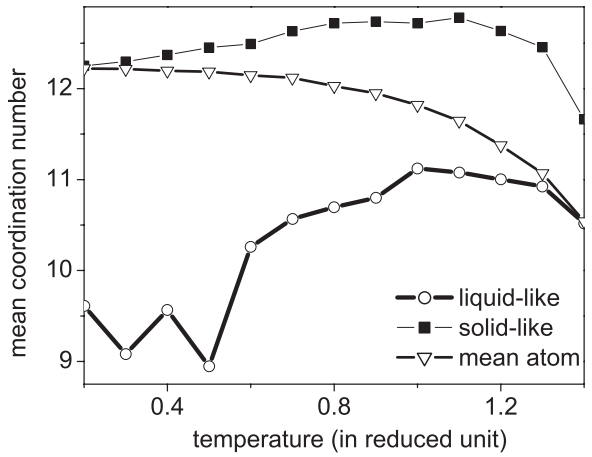

FIG. 9. Temperature dependence of the mean coordination number of solidlike and liquidlike atoms compared to that of the mean coordination number for all atoms in the system.

contrast, the mean coordination number of liquidlike atoms is close to that of all atoms at a high temperature, and it is always less than that for all atoms. This shows clearly that liquidlike atoms are often located in the non–close-packed atomic arrangement regions, which can be considered structural defects in glass. Indeed, atoms of non–close-packed atomic arrangement regions in a glassy matrix are less stable, so it is easy for them to escape from non–close-packed atomic arrangement regions to diffuse. Thus, they become liquidlike atoms via thermal vibrations. Strong fluctuations of the mean coordination number for liquidlike atoms in glassy models obtained at a temperature below $T_g = 0.61$ can be seen (Fig. 9). Due to their small population in the glassy state at a low temperature, the statistics may not be good.

IV. CONCLUSIONS

We have carried out MD simulations of glass formation in simple monatomic supercooled liquids with free surfaces. Some conclusions can be drawn:

(1) The atomic mechanism of glass formation in supercooled liquids with free surfaces shares some trends observed previously in the bulk. However, it exhibits heterogeneous behavior, unlike the homogeneous behavior observed in the bulk;[71,73] i.e., the solidlike domain initiates/enhances in the interior and simultaneously grows outward to the surfaces.

(2) Glass with free surfaces has two distinct parts: the interior and the surface shell. The former has a layer structure; layering and density of the interior are enhanced with decreasing temperature. A layer structure exists for the whole temperature range studied, from the normal liquid region into the deep glassy region. It is new since the layer structure of the density profile often disappears at high temperatures.[80,81] The interior exhibits slightly a higher density and stronger local icosahedral order compared to those in the bulk. In contrast, the surface shell has a porous structure and contains a large number of undercoordinated sites, which can play an important role in various surface phenomena of freestanding films like those found in practice.

(3) Free surfaces greatly enhance dynamics in the system, leading to a strong reduction of the glass transition temperature compared to that of the bulk. The existence of a high-mobility surface layer of the system (i.e., its thickness and the discrepancy between atomic mobility in the surface and that in the interior) has a tendency to increase with temperature.

(4) Liquidlike atoms in the glassy state, although they distribute throughout the system, have a tendency to concentrate in the surface shell. However, at a temperature just below T_g, liquidlike atoms do not form a purely liquidlike surface layer but rather form a mixed phase with equal concentrations of liquidlike and solidlike atoms. This finding clears the debate about the existence of glass with a liquidlike surface layer.[6]

(5) Although our simulation procedure does not fully emulate the main features of the laboratory vapor-deposited glass formation processes, we can infer some features of the origins of high stability of stable glass first obtained by the Ediger group. It was proposed that the formation of stable glass is enabled by surface-enhanced molecular mobility of a growing-vapor–deposited glass film. Indeed, the existence of a high-mobility surface of the system with free surfaces is found. During glass formation, free surfaces can reorganize the whole system since every atom in the system, at some time, can be part of a mobile surface layer. Due to the free surfaces, almost all atoms in the system have more freedom, and their mobility is greatly enhanced compared to that in the bulk. Therefore, they have time to find the low-energy packing configurations of high stability during a relatively slow cooling process, leading to the formation of a "practical stable" glassy state.

ACKNOWLEDGMENTS

V.V.H. thanks the Vietnam National Foundation for Science and Technology Development for the financial support under Grant No. 103.02.12.09 and G. Lauriat for the invited professorship at the Paris-Est University and for providing helpful comments to improve the work. We used visual molecular dynamics software (Illinois University) for 3D visualization of atomic configuration in the paper.

*vvhoang2002@yahoo.com

[1] J. L. Keddie, R. A. L. Jones, and R. A. Cory, Europhys. Lett. **27**, 59 (1994).

[2] J. A. Forrest, K. Dalnoki-Veress, J. R. Stevens, and J. R. Dutcher, Phys. Rev. Lett. **77**, 2002 (1996).

[3] Y. Liu, T. P. Russell, M. G. Samant, J. Stohr, H. R. Brown, A. Cossy-Favre, and J. Diaz, Macromolecules **30**, 7768 (1997).

[4] R. Jones, Curr. Opin. Colloid Interface Sci. **4**, 153 (1999).

[5] Y.-K. See, J. Cha, T. Chang, and M. Ree, Langmuir **16**, 2351 (2000).

[6] R. A. L. Jones, Nat. Mater. **2**, 645 (2003).

[7] C. J. Ellison and J. M. Torkelson, Nat. Mater. **2**, 695 (2003).

[8] C. Y. Kwong, A. B. Djurisic, V. A. L. Roy, P. T. Lai, and W. K. Chan, Thin Solid Films **458**, 281 (2004).

[9]Y. Huang and D. R. Paul, Polymer **45**, 8377 (2004).
[10]N. Tomczak, R. A. L. Vallee, E. M. H. P. van Dijk, L. Kuipers, N. F. van Hulst, and G. L. Vancso, J. Am. Chem. Soc. **126**, 4748 (2004).
[11]R. D. Priestley, C. J. Ellison, L. J. Broadbelt, and J. M. Torkelson, Science **309**, 456 (2005).
[12]Z. Fakhraai and J. A. Forrest, Phys. Rev. Lett. **95**, 025701 (2005).
[13]M. Alcoutlabi and G. B. McKenna, J. Phys. Condens. Matter **17**, R461 (2005).
[14]M. K. Mapes, S. F. Swallen, and M. D. Ediger, J. Phys. Chem. B **110**, 507 (2006).
[15]B. M. Besancon, C. L. Soles, and P. F. Green, Phys. Rev. Lett. **97**, 057801 (2006).
[16]R. A. Riggleman, K. Yoshimoto, J. F. Douglas, and J. J. de Pablo, Phys. Rev. Lett. **97**, 045502 (2006).
[17]H. Bodiguel and C. Fretigny, Phys. Rev. Lett. **97**, 266105 (2006).
[18]S. F. Swallen, K. L. Kearns, M. K. Mapes, Y. S. Kim, R. J. McMahon, M. D. Ediger, T. Wu, and S. Satija, Science **315**, 353 (2007).
[19]C. B. Roth, K. L. McNerny, W. F. Jager, and J. M. Torkelson, Macromolecules **40**, 2568 (2007).
[20]Z. Jiang, H. Kim, X. Jiao, H. Lee, Y. Byun, S. Song, D. Eom, C. Li, M. H. Rafailovich, L. B. Lurio, and S. K. Sinha, Phys. Rev. Lett. **98**, 227801 (2007).
[21]K. L. Kearns, S. F. Swallen, and M. D. Ediger, J. Chem. Phys. **127**, 154702 (2007).
[22]S. F. Swallen, K. L. Kearns, S. Satija, K. Traynor, R. J. McMahon, and M. D. Ediger, J. Chem. Phys. **128**, 214514 (2008).
[23]K. L. Kearns, S. F. Swallen, M. D. Ediger, T. Wu, Y. Sun, and L. Yu, J. Phys. Chem. B **112**, 4934 (2008).
[24]D. Qi, Z. Fakhraai, and J. A. Forrest, Phys. Rev. Lett. **101**, 096101 (2008).
[25]S. Streit-Nierobisch, C. Gutt, M. Paulus, and M. Tolan, Phys. Rev. B **77**, 041410(R) (2008).
[26]Z. Fakhraai and J. A. Forrest, Science **319**, 600 (2008).
[27]J. R. Dutcher and M. D. Ediger, Science **319**, 577 (2008).
[28]M. K. Mukhopadhyay, X. Jiao, L. B. Lurio, Z. Jiang, J. Stark, M. Sprung, S. Narayanan, A. R. Sandy, and S. K. Sinha, Phys. Rev. Lett. **101**, 115501 (2008).
[29]S. F. Swallen, K. Traynor, R. J. McMahon, and M. D. Ediger, Phys. Rev. Lett. **102**, 065503 (2009).
[30]K. L. Kearns, S. F. Swallen, M. D. Ediger, Y. Sun, and L. Yu, J. Phys. Chem. B **113**, 1579 (2009).
[31]J. Matthiesen, R. S. Smith, and B. D. Kay, Phys. Rev. Lett. **103**, 245902 (2009).
[32]A. Serghei, M. Tress, and F. Kremer, J. Chem. Phys. **131**, 154904 (2009).
[33]S. F. Swallen, K. Windsor, R. J. McMahon, M. D. Ediger, and T. E. Mates, J. Phys. Chem. B **114**, 2635 (2010).
[34]S. Xu, P. A. O'Connell, and G. B. McKenna, J. Chem. Phys. **132**, 184902 (2010).
[35]T. Koga, C. Li, M. K. Endoh, J. Koo, M. Rafailovich, S. Narayanan, D. R. Lee, L. B. Lurio, and S. K. Sinha, Phys. Rev. Lett. **104**, 066101 (2010).
[36]K. L. Kearns, K. R. Whitaker, M. D. Ediger, H. Huth, and C. Schick, J. Chem. Phys. **133**, 014702 (2010).
[37]A. K. Kandar, R. Bhattacharya, and J. K. Basu, J. Chem. Phys. **133**, 071102 (2010).
[38]M. Sikorski, C. Gutt, Y. Chushkin, M. Lippmann, and H. Franz, Phys. Rev. Lett. **105**, 215701 (2010).
[39]K. L. Kearns, M. D. Ediger, H. Huth, and C. Schick, J. Phys. Chem. Lett. **1**, 388 (2010).
[40]K. L. Kearns, T. still, G. Fytas, and M. Ediger, Adv. Mater. **22**, 39 (2010).
[41]Z. Yang, Y. Fujii, F. K. Lee, C.-H. Lam, and O. K. C. Tsui, Science **328**, 1676 (2010).
[42]K. J. Dawson, L. Zhu, L. Yu, and M. D. Ediger, J. Phys. Chem. B **115**, 455 (2011).
[43]K. Paeng, S. F. Swallen, and M. D. Ediger, J. Am. Chem. Soc. **133**, 8444 (2011).
[44]Y. Sun, L. Zhu, K. L. Kearns, M. D. Ediger, and L. Yu, Proc. Natl. Acad. Sci. USA **108**, 5990 (2011).
[45]L. Zhu, C. W. Brian, S. K. Swallen, P. T. Straus, M. D. Ediger, and L. Yu, Phys. Rev. Lett. **106**, 256103 (2011).
[46]M. R. Mruzik, S. H. Garofalini, and G. M. Pound, Surf. Sci. **103**, 353 (1981).
[47]J. A. Torres, P. F. Nealey, and J. J. de Pablo, Phys. Rev. Lett. **85**, 3221 (2000).
[48]Q. Wang, Q. Yan, P. F. Nealey, and J. J. de Pablo, J. Chem. Phys. **112**, 450 (2000).
[49]F. Vanik, J. Baschnagel, and K. Binder, Phys. Rev. E **65**, 021507 (2002).
[50]F. Vanik, J. Baschnagel, and K. Binder, J. Non-Cryst. Solid. **307-310**, 524 (2002).
[51]T. M. Truskett and V. Ganesan, J. Chem. Phys. **119**, 1897 (2003).
[52]T. S. Jain and J. J. de Pablo, Phys. Rev. Lett. **92**, 155505 (2004).
[53]K. Yoshimoto, T. S. Jain, P. F. Nealey, and J. J. de Pablo, J. Chem. Phys. **122**, 144712 (2005).
[54]J. Ghosh and R. Faller, J. Chem. Phys. **125**, 044506 (2006).
[55]J. Mittal, J. R. Errington, and T. M. Truskett, Phys. Rev. Lett. **96**, 177804 (2006).
[56]J. D. Stevenson and P. G. Wolynes, J. Chem. Phys. **129**, 234514 (2008).
[57]J. M. Kropka, V. Pryamitsyn, and V. Ganesan, Phys. Rev. Lett. **101**, 075702 (2008).
[58]J. Ghosh and R. Faller, J. Chem. Phys. **128**, 124509 (2008).
[59]F. Calvo and D. J. Wales, J. Chem. Phys. **131**, 134504 (2009).
[60]S. Peter, H. Meyer, and J. Baschnagel, J. Chem. Phys. **131**, 014902 (2009).
[61]S. Leonard and P. Harrowell, J. Chem. Phys. **133**, 244502 (2010).
[62]S. Singh and J. J. de Pablo, J. Chem. Phys. **134**, 194903 (2011).
[63]Z. Shi, P. G. Debenedetti, and F. H. Stillinger, J. Chem. Phys. **134**, 114524 (2011).
[64]R. Malshe, M. D. Ediger, L. Yu, and J. J. de Pablo, J. Chem. Phys. **134**, 194704 (2011).
[65]E. León-Gutierrez, G. Garcia, M. Clavaguera-Mora, and J. Rodríguez-Viejo, Thermochim. Acta **492**, 51 (2009).
[66]E. León-Gutierrez, G. Garcia, A. F. Lopeandia, M. T. Clavaguera-Mora, and J. Rodríguez-Viejo, J. Phys. Chem. Lett. **1**, 341 (2010).
[67]E. León-Gutierrez, A. Sepúlveda, G. Garcia, M. Clavaguera-Mora, and J. Rodríguez-Viejo, PhysChemChemPhys **12**, 14693 (2010).
[68]M. Engel and H.-R. Trebin, Phys. Rev. Lett. **98**, 225505 (2007).
[69]T. Mizuguchi and T. Odagaki, Phys. Rev. E **79**, 051501 (2009).
[70]V. V. Hoang and T. Odagaki, Physica B **403**, 3910 (2008).
[71]V. V. Hoang and T. Odagaki, Solid State Comm. **150**, 1971 (2010).
[72]V. V. Hoang, Eur. Phys. J. D **61**, 627 (2011).
[73]V. V. Hoang and T. Odagaki, J. Phys. Chem. B **115**, 6946 (2011).

[74]K. Nishio, J. Koga, T. Yamaguchi, and F. Yonezawa, J. Phys. Soc. Jpn **73**, 627 (2004).
[75]M. Dzugutov, Phys. Rev. Lett. **70**, 2924 (1993).
[76]P. G. Debenedetti and F. H. Stillinger, Nature (London) **410**, 259 (2001).
[77]W. Kob, J. Phys. Condens. Matter **11**, R85 (1999).
[78]R. A. Rigglement and J. J. Pablo, J. Chem. Phys. **128**, 224504 (2008).
[79]F. W. Starr, S. Sastry, J. F. Douglas, and S. C. Glotzer, Phys. Rev. Lett. **89**, 125501 (2002).
[80]E. Chacon, M. Reinaldo-Falagan, E. Velasco, and P. Tarazona, Phys. Rev. Lett. **87**, 166101 (2001).
[81]H. Mo, G. Evmenenko, S. Kewalramani, K. Kim, S. N. Ehrlich, and P. Dutta, Phys. Rev. Lett. **96**, 096107 (2006).
[82]J. S. Rowlinson and B. Widom, *Molecular Theory of Capillary* (Dover, New York, 2002).
[83]J. Du and A. N. Cormack, J. Am. Ceram. Soc. **88**, 2532 (2005).
[84]K. J. Dawson, K. L. Kearns, L. Yu, W. Steffen, and M. D. Ediger, Proc. Natl. Acad. Sci. USA **106**, 15165 (2009).
[85]J. D. Honeycutt and H. C. Andersen, J. Phys. Chem. **91**, 4950 (1987).
[86]M. Miller and P. Liaw (eds.), *Bulk Metallic Glasses* (Springer, New York, USA, 2007).
[87]V. V. Hoang and N. H. Cuong, Physica B **404**, 340 (2009).
[88]F. A. Lindemann, Z. Phys. **11**, 609 (1910).
[89]V. N. Novikov, E. Rossler, V. K. Malinovsky, and N. V. Surovtsev, Europhys. Lett. **35**, 289 (1996).
[90]H. M. Flores-Ruiz, and G. G. Naumis, J. Chem. Phys. **131**, 154501 (2009).
[91]U. Buchenau and R. Zorn, Europhys. Lett. **18**, 523 (1992).
[92]B. Frick and D. Richter, Phys. Rev. B **47**, 14795 (1993).
[93]K. L. Ngai, J. Non-Cryst. Solid. **275**, 7 (2000).
[94]H. M. Flores-Ruiz, G. G. Naumis, and J. C. Phillips, Phys. Rev. B **82**, 214201 (2010).
[95]M. H. Cohen and G. S. Grest, Phys. Rev. B **20**, 1077 (1979).
[96]T. Tomida and T. Egami, Phys. Rev. B **52**, 3290 (1995).
[97]J. G. Dash, Contemp. Phys. **30**, 89 (1989).
[98]T. Egami, T. Tomida, D. Kulp, and V. Vitek, J. Non-Cryst. Solid. **156-158**, 63 (1993).
[99]M. D. Ediger, C. A. Angell, and S. R. Nagel, J. Phys. Chem. **100**, 13200 (1996).
[100]C. Donati, S. Glotzer, P. Poole, W. Kob, and S. Plimpton, Phys. Rev. E **60**, 3107 (1999).
[101]M. D. Ediger, Annu. Rev. Phys. Chem. **51**, 99 (2000).